A new algebraic water flux equation for the streamlined evaluation and design of membranes and membrane systems

Alberto Tiraferri[a], Marco Malaguti[a], Madina Mohamed[a], Mattia Giagnorio[b], Fynn Jerome Aschmoneit[c,*]

[a] *Department of Environment, Land and Infrastructure Engineering, Politecnico di Torino, Corso Duca degli Abruzzi 24, 10129 Turin, Italy*

[b] *Department of Environmental and Resource Engineering, Technical University of Denmark, Miljøvej 113, Kgs. Lyngby 2800, Denmark*

[c] *Department of Mathematical Sciences, Aalborg University, A.C. Meyers Vænge 15, 2450 Copenhagen, Denmark*

Abstract

The development of new membranes, membrane materials, and membrane-based separation processes should be accompanied by a standardization of the protocols applied for membrane characterization and for system design by the community of academic and industrial stakeholders. For example, one of the obstacles to the simple and effective use of the permeate flux equation across dense membranes is the fact that the magnitude of concentration polarization depends on the flux itself, thus complicating the estimation of the latter, given a certain membrane permeance and driving force (and, on the other hand, the estimation of the membrane permeance from flux data in the presence of solutes in the feed solution). Here, a new, streamlined equation for the calculation of the water flux in pressure-driven dense membrane processes is presented. In contrast to the classic mathematical expression of the water flux, the proposed equation is algebraic. This characteristic poses the advantage of simple calculation, whereas the classic equation needs to be solved iteratively. Non-dimensional variables for water flux, driving pressure, and mass transfer are introduced as parameters of the new equation. It is shown that membrane characterization and process design are significantly simplified by deployment of the new algebraic equation and by manipulation of the non-dimensional variables. In particular, the *algebraic water flux equation* and the non-dimensional variables address the effect of concentration polarization and relate this phenomenon directly to a decline in water flux, allowing for the definition of a *filtration efficiency*. In addition, a robust protocol for the experimental characterization of the intrinsic properties of dense membranes is discussed and the results are compared to those expected from the pure solution-diffusion model of species transport. The use of the non-dimensional variables introduced in the new algebraic equation allows simpler calculation of the solute permeability coefficient of the membranes without the need to estimate the solute concentration and the membrane-feed interface or knowledge of the feed channel mass transfer coefficient.

Keywords: algebraic water flux equation; membrane characterization; non-dimensional water flux, pressure and mass transfer; process design & optimization; reverse osmosis

1. Introduction

The design and the development of the next-generation membranes for reverse osmosis (RO), nanofiltration (NF), forward osmosis, and other separation processes based on high selectivity between water and solutes or among solutes, cannot do without robust membrane characterization protocols and transport modeling tools [1, 2, 3, 4]. In turn, the deployment of current and future membranes in high-value applications require the ability to predict system performance, chiefly membrane flux, in the presence of transport-limiting

*Corresponding author

Email address: fynnja@math.auu.dk (Fynn Jerome Aschmoneit)

phenomena, such as concentration polarization [5, 6, 7]. While significant efforts are made to synthesize new dense membranes with materials previously unimaginable, these research endeavors are often accompanied by unclear and highly differentiated characterization approaches, which limit the fair comparison between membranes, impair their adoption, and not so rarely thwart the community's confidence in their applicability. In the ideal situation, a standardized, straightforward but robust evaluation procedure including both an experimental protocol and a data modeling strategy would be applied and would allow the evaluation of clear, univocal results by all parties, from materials scientist to the final stakeholders.

In processes utilizing an applied pressure on the feed side (RO, NF), when the objective of the research is the characterization of a membranes, the approach should provide values for the intrinsic permeability coefficients of the membrane, namely, that related to water transport (also known as water permeance), A, and those related to each solute of interest, B [8, 9, 10]. According to the solution-diffusion transport model, these parameters are solely related to the membrane properties and to the interaction between the membrane and the relative species in the feed solution, and they do not depend on the experimental conditions or on the modeling strategy [11]. On the other hand, when the objective of the work is to predict water flux in a variety of engineering conditions or applications, and to support the design of such systems, the approach should provide values for the permeate flux, the system productivity, and/or the system hydrodynamics properties [12, 4]. Unfortunately, reports on membrane characterization usually include permeate fluxes and observed rejection rates which, while interesting and consequential for practical purposes, are strongly dependent on specific testing conditions [13, 14]. Also, the related tests are rarely performed under reliably representative conditions of real applications, such as pressure values, hydrodynamics conditions, recovery rates, feed composition.

One of the main obstacles for the calculation of intrinsic permeability coefficients, especially B, or for the correct predictions of water flux and relevant rejection rates in real applications, is that concentration polarization must be taken into account [15]. In fact, for conditions under which a solute concentrates significantly at the membrane-feed interface, both the permeate flux and the observed rejection will be lower than expected. Accounting for concentration polarization means knowing or being able to predict the hydrodynamics condition of the membrane housing, whether in laboratory setups or in full-scale modules [16, 17]. Moreover, when hydrodynamics conditions are identified, from the convection-diffusion equations in the feed channel follows the well-known water flux equation [18]:

$$j_w = A\left[p_f + \pi_p - \pi_f \exp\left(\frac{j_w}{k_d}\right)\right] \tag{1}$$

which is a so-called a transcendental equation, because the term j_w cannot be isolated. As such, it has to be solved iteratively, and this necessity somewhat complicates the evaluation. Such intricacy and the reliance on manual calculations often invite errors, dubious approximations, inconsistency, and significant wasted time.

An important movement has recently started to make membrane performance data and membrane evaluation results more easily findable, accessible, inter-operable, and reusable. One such attempt is the Open Membrane Database (OMD), a web-based interface that collects data about membranes worldwide and "allow the easy exploration and comparison of membrane performance, physicochemical properties, and synthesis conditions" [19]. The ODM website also includes effective explanations and calculations tools for concentration polarization and membrane performance evaluation. Another parallel project is related to the development of the so-called "membrane-toolkit", a software serving as a library of validated calculators, with thorough documentation and high test coverage with the following goals: (i) automate routine tasks around membrane investigation to save time and reduce human error, (ii) promote standardization of membrane characterization, (iii) facilitate the creation and curation of large membrane data sets.

This work fits within these ongoing efforts and its main aim is to propose and assess a simplified non-trascendental algebraic equation used to relate water flux to membrane permeance and hydrodynamic conditions in the presence of concentration polarization. The equation is grounded on the solution-diffusion model and the main hypothesis is that the water flux equation from the model can be expressed in algebraic form without loss of significant information following rational approximation. A second goal is to show how a robust experimental approach allows robust membrane characterization and assessment of how well differ-

ent membranes adhere to the solution-diffusion model. The validity of the simplified water flux equation is thus evaluated under an ample range of working conditions and tested against the results of experimental characterization.

2. The algebraic water flux equation

2.1. Dimension-less numbers for filtration efficiency, pressure modulus and transportiveness

The algebraic water flux equation presented in this section is an approximation to equation 1 in terms of dimension-less numbers. These non-dimensional numbers allow for a better comparability of membrane processes, as will be shown later. The *filtration efficiency* J is defined as the ratio of the absolute water flux and the ideal water flux without concentration polarization. Depending on the magnitude of the concentration polarization, the *filtration efficiency* assumes a value between 0% and 100% and therefore poses a quantity for assessing the efficiency of the filtration process. The *pressure modulus* P is defined as the ratio of the net driving pressure and the feed osmotic pressure, which is positive for pressure driven processes. Finally, the *transportiveness* K is a measure for effectiveness of mixing in the feed channel. It is defined as the mass transfer coefficient, divided by the theoretical counter flow. A large *transportiveness* indicates good solute mixing. Only in the case of very saline solutes and at slow cross flow rates, may the *transportiveness* be smaller than unity.

$$J = \frac{j_w}{A(p_f + \pi_p - \pi_f)}, \quad P = \frac{p_f + \pi_p - \pi_f}{\pi_f}, \quad K = \frac{k_d}{A\pi_f} \tag{2}$$

2.2. Equations for process design and membrane characterization

The dimension-less numbers above are used to derive simpler expressions for the water flux and related quantities. The equations presented in this section are based on the mathematical derivation, which is found in the appendix.

Equation 3 represents the non-dimensional version of the classical water flux equation 1. This equation is in itself not simpler, nor more expressive as the classical water flux equation, since it remains a transcendental equation of the *filtration efficiency*. However, it states that the efficiency is one minus the very right-hand term, which can therefore be directly linked to the effect of concentration polarization. In the limit of perfect solute mixing, $K \to \infty$, the concentration polarization terms becomes zero and the *filtration efficiency* equation reduces to $J = 1$. That relates to $j_w = A(p_f + \pi_p - \pi_f)$, i.e. a perfect *filtration efficiency* with no concentration polarization [11].

$$J = 1 - \underbrace{\frac{1}{P}\left[\exp\left(\frac{JP}{K}\right) - 1\right]}_{\text{concentration polarization}} \tag{3}$$

The fundamental problem with this equation is its transcendental character, where the *filtration efficiency* J is both on the left hand side and inside the exponential function. The following equation is an approximation of equation 3, where the *filtration efficiency* J stands isolated on the left hand side. In contrast with the classic water flux equation, this equation is algebraic, which can be conveniently solved, without the need for iterative solvers. It is shown in Figure 1 and in the results section, that the algebraic water flux equation 4 is an excellent approximation to the original water flux equation. Similarly to the classical equation, it seen that the concentration polarization term disappears, as we assume perfect mixing, $K \to \infty$. It must be emphasized that the algebraic water flux equation is not a novel filtration model. Since it is an approximation to the classical water flux equation, it is still based on the classical convection-diffusion model.

$$J = 1 - \underbrace{\frac{1}{1+K} - \frac{PK}{2(1+K)^3}}_{\text{concentration polarization}} \tag{4}$$

In this form, the algebraic water flux equation expresses the *filtration efficiency* as 'one minus the effect of concentration polarization', that makes it especially convenient for the analysis of membrane processes. Suppose that a lab experiment or that a system is designed with $P = 3$ and $K = 7$, yielding a *filtration efficiency* of $J \approx 85\%$. That directly implies that 15% efficiency is lost to concentration polarization. Section 4 presents a detailed account on how the algebraic water flux equation is used in characterization and experiment design while Figure 1a displays the relative error resulting in applying the algebraic equation compared to the classic water flux equation. There are two distinct regions, where the algebraic water flux equation produces inaccuracies. These regions relate directly to the two assumptions involved in the derivation of the water flux equation, where the region $R_1 = (P > 5, K > 3)$ relates to assumption 1 and the region $R_2 = (K < 3)$ relates to assumption 2, see appendix. Inaccuracies in R_1 are insignificant, since the range of applicable P values does not extend over the presented range. The inaccuracies in R_2, however, become significant and overwhelming below a certain threshold, where the error contours indicate a steep increase as $K \to 0$. The region of severe inaccuracies is well captured by an empirically found threshold $4P = K(1 + K)^2$. This allows to define a practical condition for the validity of the algebraic water flux equation, $4P > K(1 + K)^2$. The orange-shaded region in Figure 1a indicates the region where the algebraic water flux equation is not valid and should not be applied. In practical terms, the condition basically renders the water flux equation invalid for diminishing cross flows only. This limitation is of little practical significance and hence, the new equation accurately reproduces the prediction of water flux of the classic equation in a wide range of P and K. Figure 1b present exemplifications of the position of the error contours for three typical dense membrane applications, namely, seawater, brackish water, and wastewater desalination. Below the respective contours in the k_d vs. p_f plots, the error is below the value indicated near each boundary. Note that the values of k_d corresponding to the 5% boundary are low compared to commonly adopted values of the mass transfer coefficient, given that the hydrodynamic regime in real systems is usually turbulent or near-turbulent. In summary, only when concentration polarization is very high, the algebraic equation is not accurate. However, such conditions are rarely found in real or in laboratory applications [20].

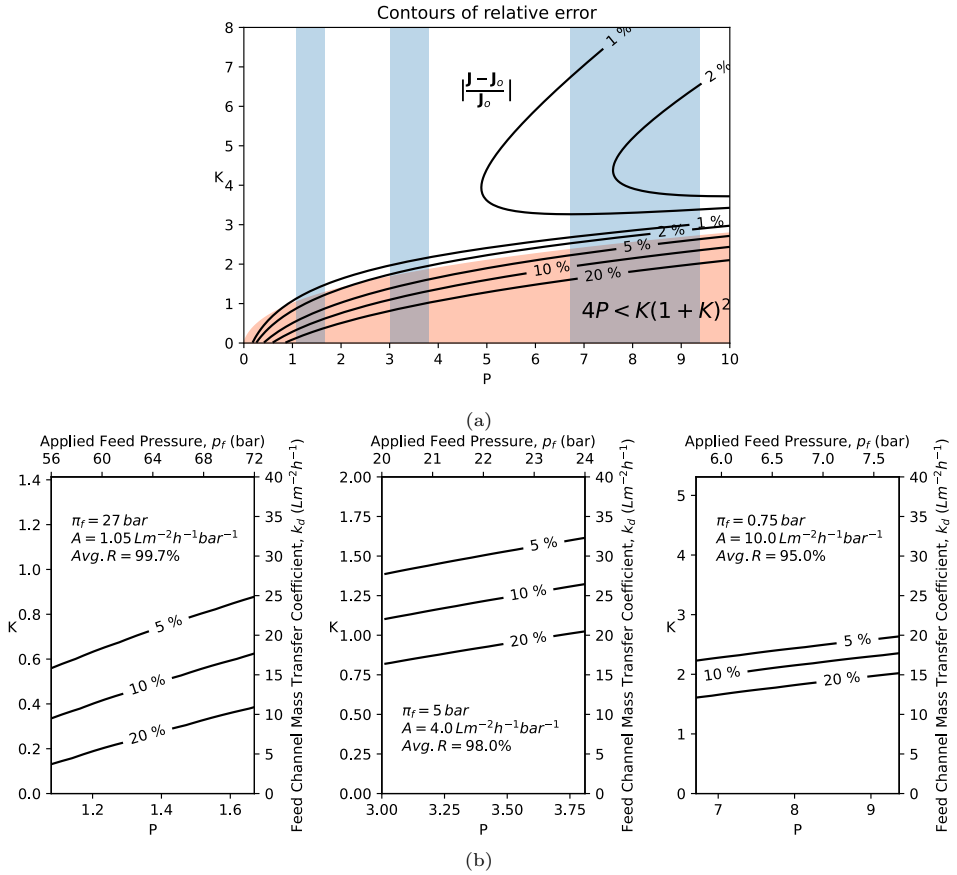

Figure 1: **Comparison with classic equation and validity in exemplary applications.** (a) Relative difference (%) between the results of water flux, J_0 obtained from original water flux equation 3 and the values of water flux, J, obtained with new water flux equation 4. (b-d) Exemplary combinations of p_f & k_d (or P & K) for typical dense membrane applications showing the contours below which the error between the algebraic and the classic equations is below a certain value. The three exemplary applications are: (a) seawater desalination using a membrane similar to SW-2; (b) brackish water desalination using a membrane similar to BW-1; (c) wastewater desalination and reuse using a membrane similar to NF.

The mass transfer coefficient k_d is a complex quantity in the sense that its value depends on the operation condition, through the cross flow velocity, the feed concentration and the solvent's diffusion coefficient, but also on the membrane geometry, through channel widths, spacers, fouling, etc [21]. A reasonable estimate for the mass transfer can be written as a function of the other process variables. Similarly, within the framework of the dimension-less process variables, the *transportiveness* K can be expressed as a function of the *filtration efficiency* J and the *pressure modulus* P as:

$$K = \frac{JP}{\ln(\underbrace{1 + P(1-J)}_{CP_{mod}})} \tag{5}$$

This expression for the *transportiveness* follows directly from the classical, non-dimensional water flux equation 3, see derivation in the appendix. It is therefore not an approximation and no errors are introduced. The argument in the logarithm function of 5 is identified as the concentration polarization modulus π_m/π_f, which yields this very simple expression the concentration polarization modulus:

$$CP_{mod} = 1 + P(1 - J) \tag{6}$$

Both, CP_{mod} and K are quantities describing the general impact of the concentration polarization on the process. Note that CP_{mod} and K are determined without knowledge of osmotic pressure at the membrane π_m. On the contrary, equation 6 can be used to estimate π_m in a simple manner.

3. A robust protocol for the experimental characterization of dense membrane transport

The intrinsic transport properties of various polyamide membranes characterized by active layers of different density were evaluated using a laboratory-scale cross-flow unit [22]. The unit comprises a high-pressure pump, a feed tank, a flat membrane housing cell, and a chiller with heat exchanger coils immersed in the feed tank for temperature control. The effective membrane active area was 20.1 cm^2 and the temperature was constant at 23 ± 0.5 °C. Membranes suitable for processes classifiable as seawater reverse osmosis (SW), brackish water reverse osmosis (BW), and nanofiltration (NF) were deployed. Prior to each experiment, the membrane sample was immersed in water overnight. The filtration tests consisted of two different phases: initially, deionized water was used as feed solution to evaluate the intrinsic water permeability coefficient of the membrane, A, (also known as water permeance); subsequently, an appropriate volume of NaCl stock solution (stock solution concentration = 5 mol/L) or of $MgSO_4$ stock solution (1 mol/L) was directly added into the feed tank to evaluate the solute permeability coefficient, B. The pH was fixed at 8.0 by addition of a minimal amount of buffer compound ($NaHCO_3$) and via adjustment with NaOH. The solute concentrations were consistent with those typically utilized by membrane manufacturer for standard membrane testing and commonly reported in the specification sheets.

In the first phase, the applied feed pressure, p_f, was changed to obtain different values of the water flux as a function of p_f. In the second phase, both p_f and the cross-flow velocity (cfv) were changed to obtain different measurements of the permeate flux and of the solute rejection. Three cfv values were investigated referred to as high, medium, and low cfv. The values of p_f and solute concentration were chosen according to the density of the membranes, higher for the denser membranes and lower for the ones with lower expected rejection. All the testing conditions can be found in Table 1. According to the solution-diffusion model, the observed rejection, R, is a function of applied feed pressure and is also affected by concentration polarization, which, in turn, is influenced by hydrodynamics conditions, e.g., cross-flow velocity. However, B is a univocal parameter for each solute, being related solely to the properties of the membrane active layer and its interaction with the solute of interest [23].

Table 1: Experimental conditions for the characterization of the six membranes

Membrane	Compaction	Phase 1		Phase 2					
	Applied pressure (bar)	Feed Solution	Applied feed pressures (bar)	Feed solution (pH 8.0)	Step 1 p_f (bar) cfv (cm/s)	Step 2 p_f (bar) cfv (cm/s)	Step 3 p_f (bar) cfv (cm/s)	Step 4 p_f (bar) cfv (cm/s)	Step 5 p_f (bar) cfv (cm/s)
SW-1	65	deionized water	55, 45, 35	32 g/L NaCl	***55*** 5.74	***55*** 2.87	***45*** 5.74	***45*** 2.87	***35*** 1.44
SW-2	65		55, 45, 35	32 g/L NaCl	***55*** 5.74	***55*** 2.87	***45*** 5.74	***45*** 2.87	***35*** 1.44
SW-3	65		55, 45, 35	32 g/L NaCl	***55*** 5.74	***55*** 2.87	***45*** 5.74	***45*** 2.87	***35*** 1.44
BW-1	20		15.5, 10, 5	2 g/L NaCl	***15.5*** 5.74	***15.5*** 2.87	***10*** 5.74	***10*** 2.87	***5*** 0.77
BW-2	10		8.6, 4.3, 3	2 g/L NaCl	***8.6*** 5.74	***8.6*** 2.87	***4.3*** 5.74	***4.3*** 2.87	***3*** 0.77
NF	6		4.3, 3.4, 2	2 g/L NaCl / 2 g/L $MgSO_4$	***4.3*** 5.74	***4.3*** 2.87	***3.4*** 5.74	***3.4*** 2.87	***2*** 0.77

In the beginning of each test, the membrane sample was compacted with DI water as feed solution at the highest value of applied pressure until the permeate flux reached a steady-state [24]. In this first phase involving deionized water as feed solution, p_f was then lowered in a step-wise fashion. In each step, the water volume passed through the membrane was measured by means of a computer-interface balance; see also Figure2a for an example of experimental data related to membrane "SW-1". The pure water flux was calculated by dividing the volumetric permeate rate, obtained at steady-state, by the membrane active area. A was determined as the slope of the best fitting line for the water flux data as a function of p_f, with the line passing through the origin (Figure 2b). In the second phase, after addition of solute in the feed solution, different steps involved operating conditions consisting of five different combinations of the same values of p_f investigated in the first phase and of the three cfv (Table 1). Solute concentrations in the feed and permeate streams were calculated from conductivity values measured using a conductivity meter (Oakton CON 450), calibrated for each salt. The permeate flux, j_w, was calculated by dividing the volumetric permeate rate by the membrane area. R, was then computed from the concentrations determined in bulk feed, c_f, and in the permeate stream, c_p, as

$$R = 1 - \frac{c_p}{c_f} \tag{7}$$

The observed rejection and the permeate flux were always measured at steady state. Therefore, within each step, i.e., for each combination of p_f and cfv, the values of these parameters were always constant in time, within experimental error. Two separate measurements were performed, distanced 10-20 min from each other and the values were averaged. Except for collection periods, both the concentrate and the permeate streams were recirculated back into the feed tank.

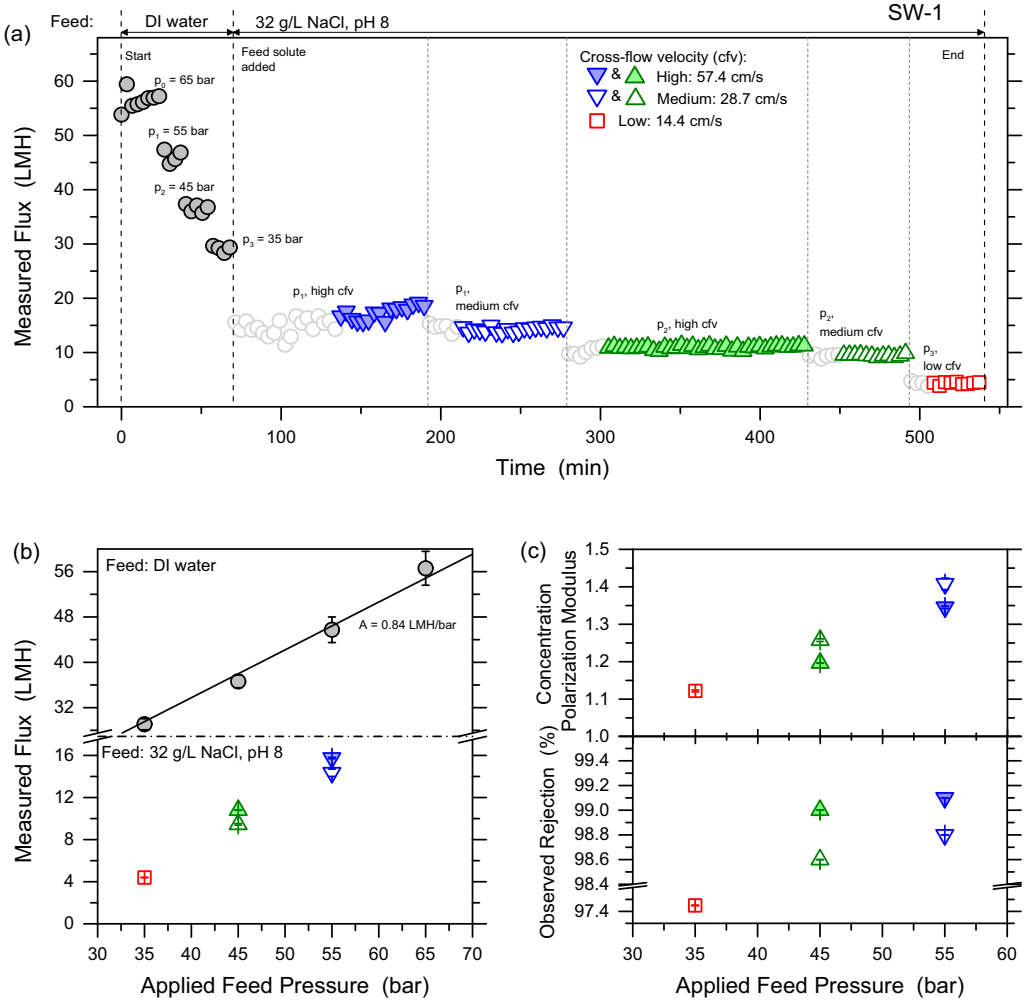

Figure 2: **Results of characterization experiment performed with representative seawater reverse osmosis membrane, SW-1, at near 0% recovery rate.** (a) Measured flux as a function of time, showing the various phases and steps. Phase 1 with deionized water as feed solution; phase 2 with 32 g/L NaCl as feed solution (pH 8.0). Empty circles in phase 2 refer to stabilization periods upon changes in feed pressure or cross-flow velocity. (b) Average and standard deviation of flux data measured in the various phases and steps, as a function of applied feed pressure; note that the y-axis has a break from 18 to 28 $\mathrm{Lm^{-2}h^{-1}}$ (LMH). (c) Average and standard deviation of (bottom) observed rejection (%) and (top) concentration polarization modulus, computed for the various steps in phase 2, as a function of applied feed pressure. Note that the y-axis of the inset related to the observed rejection has a break from 97.6 to 98.4%. In all graphs, grey circles refer to deionized water as feed solution, downward blue triangles to steps with saline feed solution and feed pressure of 55 bar, upward green triangles to steps with saline feed solution and feed pressure of 45 bar, red squares to a step with feed pressure of 35 bar and low cross-flow velocity. For the two higher pressure values, colored symbols refer to high cross-flow velocity while empty symbols to medium cross-flow velocity. Values plotted in (b) and (c) were obtained from individual data values, all under steady state conditions. The temperature was constant at 23 ± 0.5 °C.

B, was computed from experimentally available data with the following protocol. J and P were calculated from the input or measured data of the experiment. Then, equation 6 was applied to calculate the concentration polarization modulus. Finally, B was calculated as:

$$B = \frac{j_w \pi_p}{(CP_{mod}\pi_f - \pi_p)} \tag{8}$$

which is obtained by substituting equation 6 into the definition of B:

$$B = \frac{j_s}{(c_m - c_p)} = j_w \frac{c_p}{(c_m - c_p)} = j_w \frac{\pi_p}{(\pi_m - \pi_p)} \tag{9}$$

This equation does not require direct estimation of the concentration or osmotic pressure at the feed-membrane interface from experiments, with the inevitable inaccuracies related to this latter method, but instead it deploys readily available parameters, J and P included in the proposed algebraic equation. Note that B could also be computed if the value of the mass transfer coefficient, k_d, is known, with the following equation:

$$B = j_w \frac{1 - R}{R} \exp\left(\frac{j_w}{k_d}\right) \tag{10}$$

This equation is once again transcendental, thus only solved through numerical or iterative methods. Also, while k_d may be estimated from empirical relationships if the geometry of the system and the cfv are known, its value is not completely independent of the value of water flux and it is the opinion of the authors that the experimentally-based protocol for the calculation of B represents a more straightforward and robust approach. Note that in this study, the value of k_d estimated from empirical relationships was often significantly different and typically lower ($-$5-50%) compared to the k_d value that was back-calculated by reversing equation 10 and inserting the value of B obtained with equation 9. This discrepancy tended to increase with decreased membrane active layer rejection capability.

4. Results and discussion

4.1. Results of experimental membrane characterizations

Figure 2 presents the experimental results obtained with SW-1, as representative membrane. Figure 2a shows the water flux data measured as a function of time in the various phases and steps of the experiment. The average water flux data obtained at steady state is thus reported in Figure 2b as a function of p_f, where the best fitting line passing through the origin is shown for the calculation of A from flux values measured in the initial phase of the test. Figure 2c presents the values of CP_{mod} and R (NaCl) evaluated in the five steps of the second testing phase as a function of p_f, in the presence of 32 g/L NaCl in the feed solution (pH 8.0). As expected from theoretical considerations, the permeate flux increased with increasing feed pressure. Consequently, the observed NaCl rejection and the CP modulus also increased. More interestingly, flux and rejection data increased slightly but significantly with increasing cfv at a given value of p_f, thus the value of CP_{mod} decreased. Higher cfv increasing the mixing in the feed channel, reducing the thickness of the unmixed boundary layer and reducing the magnitude of external concentration polarization [25]. This phenomenon translated into a lower solute concentration at the feed-membrane interface, $c_{f,m}$, which in turns allows a higher effective driving force and lower salt passage across the membrane active layer. These observations were consistently achieved for all membranes, suggesting the reliability of the experimental protocol and the accordance between experimental results and conceptual understanding of the phenomena underlying mas transport across dense membranes [18].

Figure 3 summarizes the results in terms of A and B for all membrane types. The data are plotted for the six membranes, from the least permeable to the most permeable from left to right. As expected the highest productivity is achievable with NF membranes, followed by BW and SW membranes, respectively. The values of B correlate well with those of the parameter A, except for SW-2, which displayed both better productivity and rejection rate than SW-1. Note that the value of B estimated for NaCl with the NF membrane is significantly higher than that estimated for $MgSO_4$, since the latter solute consists of a divalent cation, thus associated with better rejection [26]. More importantly, note that the standard deviations for the parameter B are relatively small, i.e., low coefficient of variation, despite the fact that these are average of the five different steps conducted at varying feed pressure and cfv combinations. While R values changed in the five steps, B should be constant, as in fact obtained in this study.

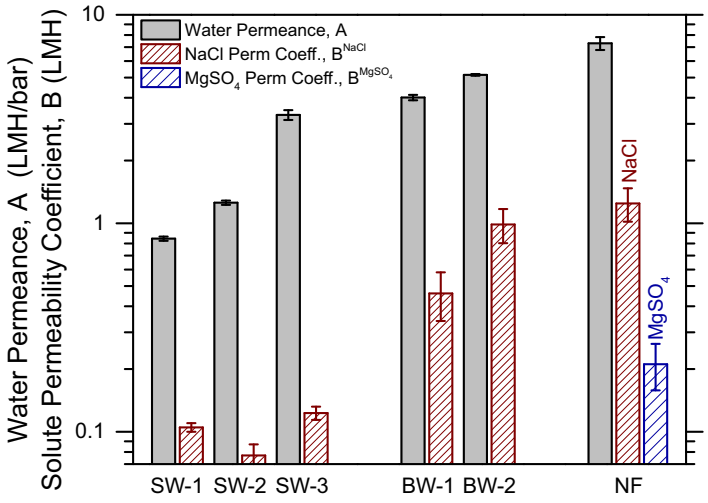

Figure 3: **Intrinsic transport parameters, A and B, computed from experimental values for the six membranes, from the least permeable to the most permeable from left to right**. Grey solid bars refer to A, while patterned bars to B. All membranes were tested in the presence of NaCl in the feed solution, except the NF membrane, which was also tested in the presence of $MgSO_4$ in the feed solution. Note that the y-axis is in logarithmic scale.

4.2. Analysis of the filtration efficiency using the algebraic water flux equation

Figure 4 shows the experimental data in the framework of the dimension-less variables. The curves are contours of the *pressure modulus* in a J-P map, calculated with the algebraic water flux equation. The experimental data are plotted in the corresponding color code, consistent with Figure 2. Apart from the SW-3 data, all data reside in regions where the accuracy of the algebraic water flux equation is at least 99% (97% for the BW-1 membrane). Hence, the figure indicates how well the experimental data adheres to the solution-diffusion model of transport and to the convection-diffusion model of polarization, as well as how robust the data are in terms of experimental estimation of the hydrodynamics parameters.

A first take-home message from the graphs is that the experimental data are much more in line with the pure solution-diffusion model as the density of the membrane active layer increases. Note that the scale of the y-axis is different for the various graphs, with SW-1, SW-2, SW-3 utilizing a smaller range of J. This result is consistent with theoretical expectations, since mechanisms of partition of the solvent and of the solutes in the membrane and their diffusion across the active layer become relatively less important compared to other mechanisms of transport, e.g., Donnan exclusion, as the ratio between species and membrane pores is reduced [27]. Even more importantly, in this work the model was computed assuming that the reflection coefficient is equal to 1, i.e., impermeable solute, which is only a fair approximation for high-rejection membranes [28]. Note that the experimental data almost always sits above the theoretical curves for all membranes, i.e., higher J values, and that for the NF membrane the consistency of the data with the theoretical curves improves for $MgSO_4$ compared to NaCl. Both these observations indicate that higher rejection rates undoubtedly allow the applicability of the pure solution-diffusion model and safely neglecting the reflection coefficient. When considering the effect of K, namely, of cross-flow velocity, note that the width of the horizontal error bars imply a certain uncertainty in accurately estimating the value of the mass transport coefficient, one of the main obstacles of membrane characterization, also highlighted above. However, no significant effect is observed in terms of correspondence between experimental data and predictions for the pure solution-diffusion model as a function of K.

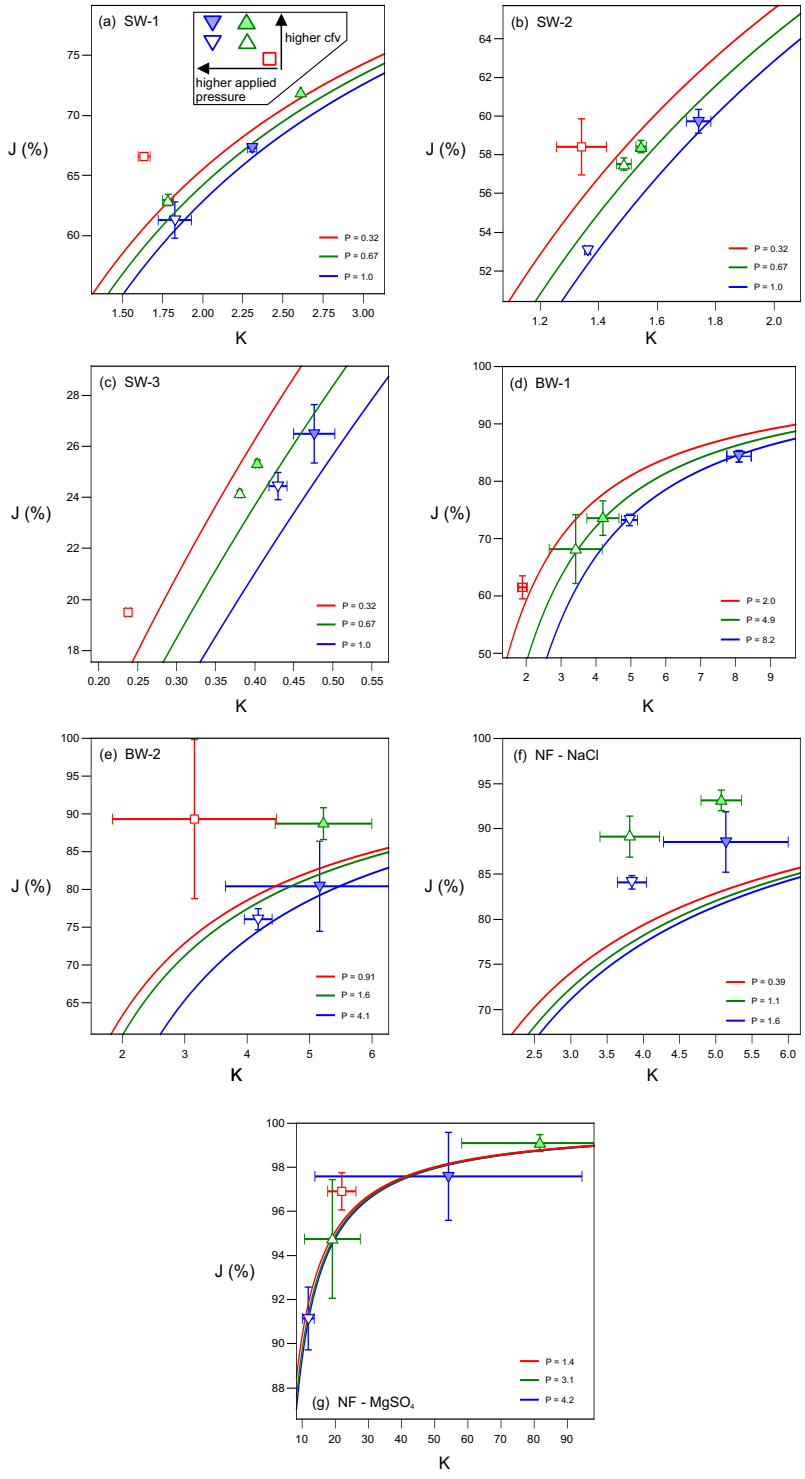

Figure 4: **Experimental results plotted in terms of K and J, and comparison with the pure solution-diffusion transport model.** Data are plotted for different membranes in the various graphs, namely, (a) SW-1, (b) SW-2, (c) SW-3, (d) BW-1, (e) BW-2, (f) NF with NaCl in the feed solution, (g) NF with $MgSO_4$ in the feed solution. Data points are plotted with the same symbols adopted in Figure 2. The three curves represent the results from the implementation of the algebraic equation 4 for three different values of P. The water fluxes in (c) lie within the region, where the algebraic flux equation becomes inaccurate.

Additional noteworthy conclusions can be draw by assessing the absolute values of J, which may be thought as a *filtration efficiency* or, in other words, how much of the nominal driving force actually goes into producing a water flux. Looking at the behavior of three seawater membranes (SW-1, SW-2, SW-3), all tested at the same value applied feed pressure, the *filtration efficiency* dropped dramatically from the least permeable to the most permeable membrane, despite the fact that the measured fluxes were obviously higher with the latter. This observation implies that attempting to increase productivity above a certain range by applying a high applied feed pressure, produces only marginal returns, as the increase in flux brings about a sustained concentration polarization that in turn limits the flux increase itself. Therefore, the energy expense associated with higher feed pressures is not entirely justified, implying that the driving force should be adjusted for each membrane permeance to be within a certain range, if the goal is to improve efficiency. In real applications, the system productivity is often set by the needs of an industry or a community and the degree of freedom in that respect may be lower. However, the results of this study suggest that an increase in membrane area may be more advantageous that that of applied feed pressure, to maintain overall productivity while increasing efficiency. Indeed, economic considerations are outside the scope of this study and must be taken into consideration. As the values of applied feed pressure were adjusted sequentially for more and more permeable membranes (NF > BW-2 > BW-1 > SW),it was possible to restore *filtration efficiency* by working at the appropriate range of flux to limit concentration polarization.

4.3. Application of the algebraic equation in process design and membrane characterization

Figure 5 presents sensitivity maps from the implementation of equations presented above in terms of various interdependencies among K, P, J, and CP_{mod}. Specifically, Figure 5a is a map of equation 4, Figure 5d is a map of equation 6, while Figures 5b,c are alternative representations of Figures 5d,a, respectively. Several conclusions may be drawn about the strong or weak dependency of the variables on each other. For example, at a fixed value of P, the *filtration efficiency* can only be increased by increasing the mass transfer coefficient in the feed channel, hence K. On the other hand, at a fixed value of K, the *filtration efficiency* can partly be also increased by reducing P, that is, by working with a smaller driving force and a smaller overall productivity. To exemplify this discussion, a hypothetical optimization strategy may be assumed, in which an initial process with 80% *filtration efficiency* should be modified to reach a value of efficiency equal to 85%. If the process is characterized by $P = 6, K = 5.9$ (see starting point for the two arrows in Figure 5a), the ECP can be reduced by moving into different directions. The red vertical arrow relates to the case where the feed pressure is held constant and K is increased, i.e., the cross-flow velocity. The blue horizontal arrow indicates the case whereby ECP is reduced by lowering the feed pressure at constant cross-flow. However, Figure 5a suggests that the effect of K is more significant in influencing J than that of P. A strategy for optimizing a process in terms of *filtration efficiency* would thus favor adjusting the cross-flow velocity rather than the pressure. Similar to Figure 1a, the orange region indicates ranges in P and K, for which the water flux equation is invalid. It can be seen that the threshold coincides well with the 50% efficiency contour. From that a rule of thump can be defined on the applicability: The algebraic water flux equation is valid for calculated efficiencies of 50% and more.

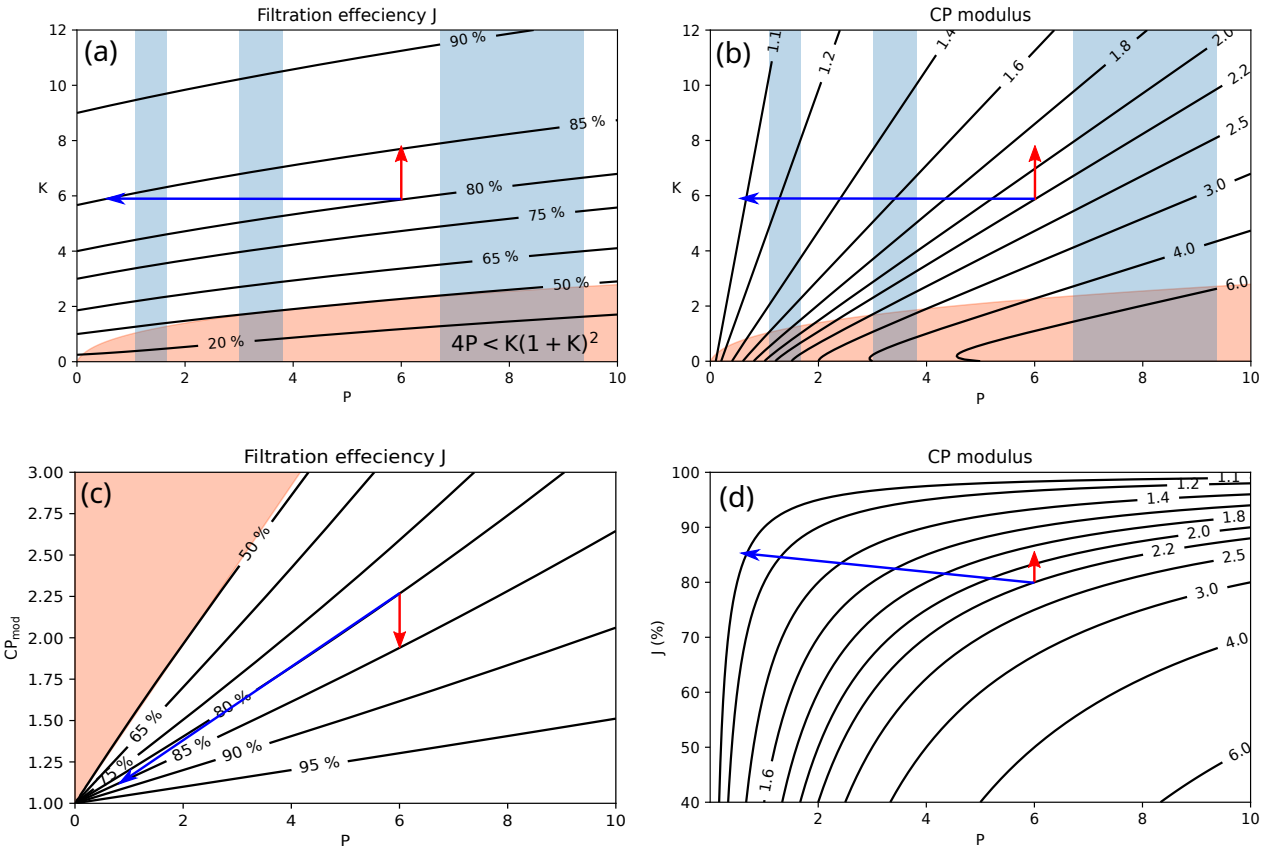

Figure 5: **Sensitivity analyses of filtration efficiency and concentration modulus** (a,c) contour plots of *filtration efficiency* J as a function of the *pressure modulus* P and the *transportiveness* K (a) or the concentration modulus CP_{mod} (c). (b,c) contour plots of the concentration modulus for *pressure modulus* and *transportiveness*(b) of *filtration efficiency*(d). The red shaped regions refer to operation variables, for which the algebraic water flux equation is not valid. The blue shaded regions refer to typical application values for the *pressure modulus*, as defined in Fig1. The arrows depict two hypothetical optimization scenarios.

Figures 5b,d indicate how the CP modulus changes in the same optimization process: The initial process with 80% efficiency has a CP_{mod} of 2.2. When reducing the feed pressure at constant cross flow (blue leftward arrow), the CP_{mod} drops to 1.1 when we reach a *filtration efficiency* of 85%. In the case of increasing cross-flow at constant feed pressure, the CP_{mod} is instead reduced from 2.2 to 1.9. This observation implies that reducing the CP_{mod} can be very efficiently done by lowering the feed pressure, while increasing the cross-flow only has a limited effect. Note that the two outcomes in Figure 5a and Figure 5d are not in contradiction, but they actually suggest something less than trivial and related to the definition of *filtration efficiency* and CP_{mod}. J is a better parameter for assessing the impact of ECP, i.e., the process, while the CP_{mod} is an efficiency related to how rationally the membrane is being deployed. Figures 5c,d indicate the relation of the *filtration efficiency* and the concentration modulus. CP_{mod} indicates how much concentration exist at the membrane-feed interface, but it does not necessarily indicate how much water flux is lost with respect to ideality. On the other hand, J does not indicate what the concentration is at the membrane-feed interface, but rather how much the water flux will be reduced.

Furthermore, Figure 5 may be used to help design a membrane or a membrane system. If the goal is maintaining a high *filtration efficiency*, thus allowing the correct exploitation of a certain driving force, the combinations of P and K can be determined from the maps for a certain target value of J. Based on the membrane properties and on the needed system productivity, one can thus calculate the required values of the absolute design variables, p_{f} and k_{d}. Or alternatively, the required value of A, that is, the most appropriate

membrane for a certain application, can be estimated to achieve a certain fixed productivity or *filtration efficiency*, known or hypothesized the operating conditions of a system.

4.4. Implication for membrane systems

Having a simple equation that allows for the calculation of the water flux across dense membranes would simplify preliminary system design and predictions around productivity. The deployment of the equation proposed in this study allows for the streamlined exploration of a wide range of operating conditions to achieve a first useful approximation of the potential functioning of a system deploying a particular membrane. On the other hand, it also promotes understanding of the functioning of different membranes in a specific system, with implications about the rational choice of a membrane with suitable transport parameters. This type of preliminary estimations are currently performed with the need of cumbersome iterations or with the use of specific software, which often limits the scope of the investigations and of the design efforts by membrane developers or system engineers. The algebraic equation includes non-dimensional parameters with physical meaning and it is conceived so that its terms are strongly correlated to the efficiency of the process. Indeed, the highlight of the equation terms on system efficiency and the possibility to easily estimate the magnitude of concentration polarization allow a better understanding of the performance of a system and of a membrane, beyond sole assessment of productivity. Such considerations on efficiency, namely, the optimal functioning of a system and the appropriate exploitation of a membrane to its true potential are often overlooked or disregarded, as there is a tendency to focus on flux maximization rather then flux optimization. Therefore, other than simplifying flux prediction or experimental procedures, the deployment of the algebraic equation proposed in this study may help make processes more rational.

5. Conclusions

In this work, a new algebraic equation was developed to predict water flux across dense membranes in the presence of concentration polarization. The equation includes non-dimensional numbers that allow for a better comparability of membranes and membrane processes, namely, the *filtration efficiency*, J, defined as the ratio of the absolute water flux and the ideal water flux without concentration polarization, the *pressure modulus*, P, defined as the ratio of the net driving pressure and the feed osmotic pressure, and the *transportiveness*, K, a measure for effectiveness of mixing in the feed channel. The equation is highly accurate (i.e., it does not deviate significantly from the water flux classic equation) for a wide range of K and P, and its accuracy is lost only for a combination of low K and large P vales, that is, when concentration polarization is of very high magnitude, conditions that are rarely found in laboratory or full-scale applications.

The results from the equation were also compared against a set of membrane transport data obtained by means of a robust experimental protocol including various steps of pressure and cross-flow velocity combinations. The protocol was deployed for six different membranes, from highly selective seawater RO membranes to looser NF membranes. The data from the experimentation were robust and consistent with the solution-diffusion model of membrane transport and the convection-diffusion boundary layer model of concentration polarization especially in the case of more selective membranes. For looser membranes, incorporation of the reflection coefficient in the calculations becomes critical for a accurate description of the phenomena and the proper membrane or system characterization.

The streamlined implementation of the algebraic equation promotes understanding and optimization of a membrane system in terms of efficiency of utilization of the driving force and of the membrane intrinsic potential (beside the correct prediction of water flux, hence productivity) without the need for cumbersome iterations or the use of a specialized software. Specifically, calculations using the proposed equation simplify the choice of the correct combination of K and P, thus of the mass transfer coefficient in the feed channel and of the applied feed pressure in a given system. Or, alternatively, they simplify the identification of a membrane with suitable transport properties for a certain target productivity. This work supports the current ongoing efforts aimed at simplifying and standardizing the characterization and evaluation of membrane and membrane systems, to promote further progress in this field.

Acknowledgements

M.M. would like to thank Eni S.p.A. for funding her Ph.D. scholarship.

References

[1] A. Tiraferri, N. Y. Yip, A. P. Straub, S. R.-V. Castrillon, M. Elimelech, A method for the simultaneous determination of transport and structural parameters of forward osmosis membranes, Journal of membrane science 444 (2013) 523–538.

[2] F. J. Aschmoneit, C. Hélix-Nielsen, Chapter 3 - application of computational fluid dynamics technique in reverse osmosis/nanofiltration processes, in: A. Basile, K. Ghasemzadeh (Eds.), Current Trends and Future Developments on (Bio-) Membranes, Elsevier, 2022, pp. 63–79.

[3] M. Heiranian, R. M. DuChanois, C. L. Ritt, C. Violet, M. Elimelech, Molecular simulations to elucidate transport phenomena in polymeric membranes, Environmental Science & Technology 56 (6) (2022) 3313–3323.

[4] F. J. Aschmoneit, C. Hélix-Nielsen, Omsd–an open membrane system design tool, Separation and Purification Technology 233 (2020) 115975.

[5] P. Biesheuvel, J. Dykstra, S. Porada, M. Elimelech, New parametrization method for salt permeability of reverse osmosis desalination membranes, Journal of Membrane Science Letters 2 (1) (2022) 100010.

[6] Y. Du, Z. Wang, N. J. Cooper, J. Gilron, M. Elimelech, Module-scale analysis of low-salt-rejection reverse osmosis: Design guidelines and system performance, Water Research 209 (2022) 117936.

[7] Y. S. Oren, V. Freger, O. Nir, New compact expressions for concentration-polarization of trace-ions in pressure-driven membrane processes, Journal of Membrane Science Letters 1 (1) (2021) 100003.

[8] V. Freger, G. Z. Ramon, Polyamide desalination membranes: Formation, structure, and properties, Progress in Polymer Science 122 (2021) 101451.

[9] M. Asadollahi, D. Bastani, S. A. Musavi, Enhancement of surface properties and performance of reverse osmosis membranes after surface modification: A review, Desalination 420 (2017) 330–383.

[10] R. Kingsbury, J. Wang, O. Coronell, Comparison of water and salt transport properties of ion exchange, reverse osmosis, and nanofiltration membranes for desalination and energy applications, Journal of Membrane Science 604 (2020) 117998.

[11] J. Wijmans, R. Baker, The solution-diffusion model: a review, Journal of Membrane Science 107 (1) (1995) 1–21.

[12] R. H. Hailemariam, Y. C. Woo, M. M. Damtie, B. C. Kim, K.-D. Park, J.-S. Choi, Reverse osmosis membrane fabrication and modification technologies and future trends: A review, Advances in Colloid and Interface Science 276 (2020) 102100.

[13] R. S. Kingsbury, S. Zhu, S. Flotron, O. Coronell, Microstructure determines water and salt permeation in commercial ion-exchange membranes, ACS Applied Materials & Interfaces 10 (46) (2018) 39745–39756.

[14] E. M. Van Wagner, A. C. Sagle, M. M. Sharma, B. D. Freeman, Effect of crossflow testing conditions, including feed ph and continuous feed filtration, on commercial reverse osmosis membrane performance, Journal of Membrane Science 345 (1) (2009) 97–109.

[15] J. C. Chen, Q. Li, M. Elimelech, In situ monitoring techniques for concentration polarization and fouling phenomena in membrane filtration, Advances in Colloid and Interface Science 107 (2) (2004) 83–108.

[16] B. J. Mariñas, R. I. Urama, Modeling concentration-polarization in reverse osmosis spiral-wound elements, Journal of Environmental Engineering 122 (4) (1996) 292–298.

[17] F. J. Aschmoneit, C. Hélix-Nielsen, Submerged-helical module design for pressure retarded osmosis:A conceptual study using computational fluid dynamics, Journal of Membrane Science 620 (2021) 118704.

[18] R. W. Baker, Membrane technology and applications, John Wiley & Sons, 2012.

[19] C. L. Ritt, T. Stassin, D. M. Davenport, R. M. DuChanois, I. Nulens, Z. Yang, A. Ben-Zvi, N. Segev-Mark, M. Elimelech, C. Y. Tang, G. Z. Ramon, I. F. Vankelecom, R. Verbeke, The open membrane database: Synthesis–structure–performance relationships of reverse osmosis membranes, Journal of Membrane Science 641 (2022) 119927.

[20] G. Srivathsan, E. M. Sparrow, J. M. Gorman, Reverse osmosis issues relating to pressure drop, mass transfer, turbulence, and unsteadiness, Desalination 341 (2014) 83–86.

[21] I. Sutzkover, D. Hasson, R. Semiat, Simple technique for measuring the concentration polarization level in a reverse osmosis system, Desalination 131 (1) (2000) 117–127.

[22] G. Öner, N. Kabay, E. Güler, M. Kitiş, M. Yüksel, A comparative study for the removal of boron and silica from geothermal water by cross-flow flat sheet reverse osmosis method, Desalination 283 (2011) 10–15.

[23] J. Wang, D. S. Dlamini, A. K. Mishra, M. T. M. Pendergast, M. C. Wong, B. B. Mamba, V. Freger, A. R. Verliefde, E. M. Hoek, A critical review of transport through osmotic membranes, Journal of Membrane Science 454 (2014) 516–537.

[24] D. M. Davenport, C. L. Ritt, R. Verbeke, M. Dickmann, W. Egger, I. F. Vankelecom, M. Elimelech, Thin film composite membrane compaction in high-pressure reverse osmosis, Journal of Membrane Science 610 (2020) 118268.

[25] S. Kim, E. M. Hoek, Modeling concentration polarization in reverse osmosis processes, Desalination 186 (1) (2005) 111–128.

[26] M. Park, J. Park, E. Lee, J. Khim, J. Cho, Application of nanofiltration pretreatment to remove divalent ions for economical seawater reverse osmosis desalination, Desalination and Water Treatment 57 (44) (2016) 20661–20670.

[27] A. I. Schäfer, A. G. Fane, Nanofiltration: Principles, applications, and new materials, John Wiley & Sons, 2021.

[28] H. Hyung, J.-H. Kim, A mechanistic study on boron rejection by sea water reverse osmosis membranes, Journal of Membrane Science 286 (1) (2006) 269–278.

Appendix

Derivation of the algebraic water flux equation

The non-dimensional process variables are:

$$J = \frac{j_w}{A(p_f + \pi_p - \pi_f)}, \quad K = \frac{k_d}{A\pi_f}, \quad P = \frac{p_f + \pi_p - \pi_f}{\pi_f} \tag{11}$$

The classical water flux equation is expanded:

$$
\begin{aligned}
j_w &= A\left[p_f + \pi_p - \pi_f \exp\left(\frac{j_w}{k_d}\right)\right] \\
&= A\left(p_f + \pi_p - \pi_f\right)\exp\left(\frac{j_w}{k_d}\right) - A\left(p_f + \pi_p\right)\exp\left(\frac{j_w}{k_d}\right) + A(p_f + \pi_p)
\end{aligned}
\tag{12}
$$

Dividing the above equation with $A(p_f + \pi_p - \pi_f)$ and substituting j_w/k_d with JP/K yields:

$$
\begin{aligned}
J &= \exp\left(\frac{JP}{K}\right) - \frac{p_f + \pi_p}{p_f + \pi_p - \pi_f}\exp\left(\frac{JP}{K}\right) + \frac{p_f + \pi_p}{p_f + \pi_p - \pi_f} \\
&= \exp\left(\frac{JP}{K}\right) - \left(1 + \frac{1}{P}\right)\exp\left(\frac{JP}{K}\right) + \left(1 + \frac{1}{P}\right)
\end{aligned}
\tag{13}
$$

From the above equation follows the non-dimensional form of the classic flux equation 3:

$$
J = 1 + \frac{1}{P}\left[1 - \exp\left(\frac{JP}{K}\right)\right] \tag{14}
$$

Under **assumption 1**, $JP < K$, the exponential function can be written as a series:

$$
\begin{aligned}
J &= 1 + \frac{1}{P}\left[1 - \left(1 + \frac{JP}{K} + \frac{1}{2}\left(\frac{JP}{K}\right)^2\right)\right] \\
&= 1 - \frac{1}{P}\left[\frac{JP}{K} + \frac{1}{2}\left(\frac{JP}{K}\right)^2\right]
\end{aligned}
\tag{15}
$$

$$
0 = \frac{1}{2}\frac{PJ^2}{K^2} + J\left(\frac{1}{K} + 1\right) - 1 \tag{16}
$$

Solving for J:

$$
0 = J^2 + J\frac{2K}{P}(1 + K) - 2\frac{K^2}{P} \tag{17}
$$

$$
\begin{aligned}
J &= -\frac{K}{P}(1 + K) \pm \left[\left(\frac{K}{P}\right)^2(1 + K)^2 + 2\frac{K^2}{P}\right]^{\frac{1}{2}} \\
&= \frac{K}{P}(1 + K)\left(-1 \pm \left[1 + 2\frac{P}{(1 + K)^2}\right]^{\frac{1}{2}}\right)
\end{aligned}
\tag{18}
$$

The argument in the square root is greater than one. A positive-valued water flux J is expected and therefore only the + sign is considered in the above equation. Under **assumption 2**, $2P < (1 + K)^2$, the square root can be expanded with $\sqrt{1 + \alpha} \approx 1 + \frac{1}{2}\alpha - \frac{1}{8}\alpha^2$.

$$
\begin{aligned}
J &= \frac{K}{P}(1 + K)\left(-1 + \left[1 + \frac{P}{(1 + K)^2} - \frac{P^2}{2(1 + K)^4}\right]\right) \\
&= \frac{K}{1 + K} - \frac{PK}{2(1 + K)^3} \\
&= 1 - \frac{1}{1 - K} - \frac{PK}{2(1 + K)^3}
\end{aligned}
\tag{19}
$$

which concludes the derivation of equation 4.

Derivation of concentration modulus equation

Solving the classical water flux equation for the exponent in the exponential function yields:

$$\begin{aligned}\frac{j_w}{k_d} &= \ln\left(\frac{p+\pi_p-\frac{j_w}{A}}{\pi_f}\right)\\ &= \ln\left(\frac{\pi_m}{\pi_f}\right)\\ &= \ln\left(CP_{mod}\right)\end{aligned} \tag{20}$$

Similarly, solving the non-dimensional water flux equation 14 for the argument in the exponent yields:

$$\frac{JP}{K} = \ln\left(1+P(1-J)\right) \tag{21}$$

Identifying $JP/K = j_w/k_d$ imposes that the arguments in the logarithm function must be same. From that follows:

$$CP_{mod} = 1+P(1-J) \tag{22}$$